J. Am. Chem. Soc. 1990, 112, 9148-9156

Stereoselectivity of Hydrogen 1,2-Shifts in Singlet Alkylcarbenes: A Quantitative Theoretical Assessment of Ground-State Orbital Alignment and Torsional and Steric Effects[†]

J. D. Evanseck and K. N. Houk*

Contribution from the Department of Chemistry and Biochemistry, University of California, Los Angeles, Los Angeles, California 90024-1569. Received March 19, 1990

Abstract: The influence of ground-state σ_{CH} alignment on the rates of singlet carbene hydrogen 1,2-shifts has been studied with ab initio molecular orbital theory. Geometry optimizations were performed on five model systems with restricted Hartree–Fock calculations and the 3-21G or 6-31G* basis sets. These systems are dimethylcarbene, cyclohexylidene (carbenacyclohexane), carbena-2-norbornane, carbena-2-norbornene, and brexan-5-ylidene (carbena-5-brexane). The effect of electron correlation was included with use of second-order Møller–Plesset theory with the 6-31G* basis on the optimized 6-31G* geometries. Electron correlation was found to have no effect upon the relative activation energies, which are in excellent accord with experiment. The exo selectivities observed and predicted for 1,2-shifts in rigid systems are explained by torsional and steric interactions that develop in the transition structures. Ground-state orbital alignment induces significant geometric distortions yet has little influence on the rates of rearrangements of singlet alkylcarbenes. Because the planar double-bond geometry of the product is already achieved in the 1,2-shift transition structure, there is no difference in the activation energy for axial and equatorial hydrogen migration in cyclohexylidene.

Introduction

The 1,2-shift of hydrogen in a singlet carbene to form an alkene formally involves the migration of a hydrogen to a vacant orbital. It has been proposed that the ease of this migration should be related to the ground-state alignment of the vacant and σ_{CH} orbitals.[1] Carbenes derived from norbornanes have a preferential alignment of exo σ_{CH} and vacant orbitals and have been reported to undergo stereoselective thermal rearrangements. Substituted cyclohexylidenes on the other hand have shown very little selectivity between the axial and equatorial processes, even though the axial σ_{CH} has almost perfect alignment with the vacant orbital and the equatorial has very poor alignment in the ground state. Thus, there is conflicting evidence about whether orbital alignment has any effect on activation energies.

We have undertaken theoretical studies of the geometries and reactions of several carbene systems and have determined the origins of low to moderate selectivity in these thermal rearrangements. The carbene systems studied here are dimethylcarbene, cyclohexylidene (carbenacyclohexane), carbena-2-norbornane, carbena-2-norbornene, and brexan-5-ylidene (carbena-5-brexane), which are shown in Figure 1.

Background

Nickon and co-workers carried out a series of thermal and photochemical Bamford–Stevens reactions on brexan-5-one to determine the stereochemistry of the rearrangement of brexan-5-ylidene, **1**.[2] Deuterated substrates were studied, yielding a primary isotope affect of $k_H/k_D = 1.30$ for both epimers and an exo/endo migration ratio of 138.

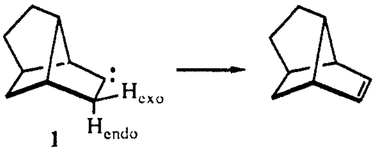

1

The norbornene derivatives **2a** and **2b** were later investigated by Kyba.[3] Analysis of the olefins from the rearrangements of deuterated derivatives yielded migratory ratios of 13 and 18, respectively.

Freeman and co-workers reported that dimethylnorbornan-2-ylidene, **3**, gave a preference of approximately 20:1 for exo migration.[4] The higher selectivity in brexan-5-ylidene than in structures **2** and **3** was rationalized as a consequence of better ground-state alignment of the exo hydrogen as a result of the geometric distortion provided by the additional alkyl tether.[2,3]

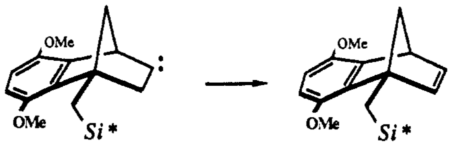

2a

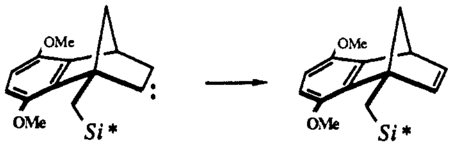

2b

Si* = *tert*-butyldimethylsiloxy

3

Kyba and John found a 1.5:1 axial:equatorial migratory ratio for *tert*-butylcyclohexylidene, **4**, with an isotope effect of k_H/k_D = 1.9 for both axial and equatorial protons.[5]

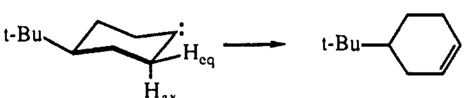

4

[†] Dedicated to Professor Wolfgang Kirmse on the occasion of his 60th birthday.

(1) (a) Jones, W. M. In *Rearrangements in Ground and Excited States*; de Mayo, P., Ed.; Academic Press: New York, 1980; pp 95–160. (b) Gaspar, P. P.; Hammond, G. S. In *Carbenes*; Moss, R. A.; Jones, M., Jr., Eds.; Wiley: New York, 1975; Vol. 11, pp 207–362.

(2) Nickon, A.; Huang, F-chih; Weglein, R.; Matsuo, K.; Yagi, H. *J. Am. Chem. Soc.* **1974**, *96*, 5264.

(3) (a) Kyba, E. P.; Hudson, C. W. *J. Org. Chem.* **1977**, *42*, 1935. (b) Kyba, E. P.; Hudson, C. W. *J. Am. Chem. Soc.* **1976**, *98*, 5696.

(4) Freeman, P. K.; Hardy, T. A.; Balyeat, J. R.; Wescott, L. D., Jr. *J. Org. Chem.* **1977**, *42*, 3356.

0002-7863/90/1512-9148$02.50/0

Table I. Energies of Methylcarbene, Dimethylcarbene, Cyclohexylidene, Carbena-2-norbornane, Carbena-2-norbornene, and Brexan-5-ylidene and the Transition States for the Rearrangements (Energies Reported in Hartrees and Zero-Point Energies (kcal/mol) in Parentheses)

species	sym	AM1	RHF/3-21G	RHF/6-31G*	MP2/6-31G*// RHF6-31G*[a]
methylcarbene	C_1	0.139 70	−77.485 09	−77.922 37 (33.7)	−78.162 06
TS H 1,2-shift	C_1	0.163 47	−77.451 89	−77.900 95 (32.8)	−78.159 27
dimethylcarbene[b]	C_s		−116.318 16	−116.970 76 (53.0)	−117.348 21
dimethylcarbene[c]	C_{2v}	0.107 99	−116.317 79	−116.969 99 (52.8)	−117.347 24
dimethylcarbene[d]	C_{2v}	0.112 12	−116.315 79	−116.968 37 (52.7)	−117.344 43
TS H 1,2-shift	C_1	0.138 96	−116.277 72	−116.940 68 (52.5)	−117.337 86
cyclohexylidene	C_s	0.085 35	−231.620 61	−232.914 40 (99.8)	−233.664 41
TS-eq	C_1	0.113 36	−231.586 85	−232.891 50 (98.2)	−233.661 88
TS-ax	C_1	0.113 04	−231.587 16	−232.891 48 (98.2)	−233.662 00
cyclohexylidene[e]	C_1	0.086 68	−231.620 60	−232.914 38	−233.664 34
TS-eq[e]	C_1	0.116 34	−231.582 57	−232.887 34	−233.658 01
TS-ax[e]	C_1	0.114-95	−231.583 97	−232.888 45	−233.659 47
carbena-2-norbornane	C_1	0.131 00	−269.281 78 (104.8)		
TS-exo	C_1	0.170 04	−269.235 88 (102.5)		
TS-endo	C_1	0.170 55	−269.232 97 (102.5)		
carbena-2-norbornene	C_1	0.195 46	−268.082 50 (88.6)		
TS-exo	C_1	0.235 68	−268.033 29 (86.2)		
TS-endo	C_1	0.235 58	−268.029 89 (86.2)		
brexan-5-ylidene	C_1	0.143 28	−345.757 29 (129.6)		
TS-exo	C_1	0.181 75	−345.712 73 (127.2)		
TS-endo	C_1	0.183 35	−345.708 31 (127.3)		

[a] The MP2 energies were determined with inclusion of the full core. Geometries were fully optimized for dimethylcarbene, methylcarbene, and corresponding transition states; otherwise single-point energy determinations were made on the optimized RHF/6-31G* geometries. [b] A C_s AM1 ground state could not be located. [c] CH eclipsed with CC. [d] CH staggered with CC. [e] Constrained ontimizations with the axial hydrogen parallel to the vacant p-orbital for the ground-state calculations. Subsequent transition states were determined with the ground-state geometry of the carbon framework held fixed.

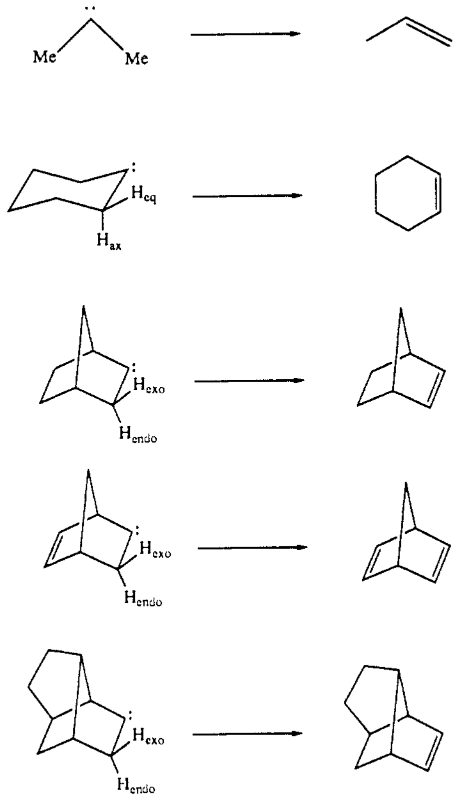

Figure 1. Reactions for which transition structures were calculated.

Press and Shechter reported that the carbene rearrangements of *cis*- and *trans*-**5** give an axial:equatorial migratory ratio of 3.2:1.[6]

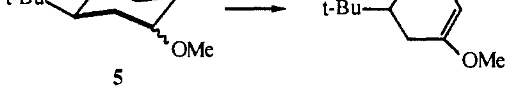

5

Seghers and Shechter have also shown that either hydrogen or phenyl migration in 2-phenyl-*cis*- and *trans*-5-*tert*-butylcyclohexylidene, **6**, occurs with little axial preference.[7]

6

The lower selectivity of substituted cyclohexylidenes complicates the arguments in support of ground-state alignment, since there is better alignment of the axial hydrogen and the carbene p-orbital in cyclohexylidenes than in norbornanylidenes.

Semiempirical calculations have been carried out to explore the effect of ground-state orbital alignment. Dewar reported a large preference for axial migration in cyclohexylidene with the MINDO/2 method.[8] With partially optimized structures, the predicted activation energy for axial migration was 1.4 kcal/mol, which is predicted to be substantially less than for the equatorial and "large enough for a rather confident prediction that rearrangement of cyclohexylidene must be highly stereospecific".[8] Altmann, Tee, and Yates also studied the same rearrangement in terms of the principle of least motion and predicted that significant axial preference should prevail.[9] Kyba later reinvestigated the cyclohexylidene rearrangement with both MINDO/3 and MNDO with fully optimized structures.[10] Both methods reveal only a slight 0.3 kcal/mol axial migration preference, in good accord with experiment, since essentially no axial preference is observed.

Theoretical Methods

All calculations were carried out with GAUSSIAN86[11] on the Digital VAX-II and VAX-2000, Harris 1000, and IBM 3090/600J computers. Geometry optimizations were carried out with RHF theory with the

---

(5) Kyba, E. P.; John, A. M. *J. Am. Chem. Soc.* **1977**, *99*, 8329.

(6) Press, L. S.; Shechter, H. *J. Am. Chem. Soc.* **1979**, *101*, 509.

(7) Seghers, L.; Shechter, H. *Tetrahedron Lett.* **1976**, *23*, 1943.

(8) Bodor, N.; Dewar, M. J. S. *J. Am. Chem. Soc.* **1972**, *94*, 9103.

(9) Altmann, J. A.; Tee, O. S.; Yates, K. *J. Am. Chem. Soc.* **1976**, *98*, 7132.

(10) Kyba, E. P. *J. Am. Chem. Soc.* **1977**, *99*, 8330.

(11) Frisch, M. J.; Binkley, J. S.; Schlegel, H. B.; Raghavachari, K.; Melius, C. F.; Martin, R. L.; Stewart, J. J. P.; Bobrowicz, F. W.; Rohlfing, C. M.; Kahn, L. R.; DeFrees, D. J.; Seeger, R.; Whiteside, R. A.; Fox, D. J.; Fleuder, E. M.; Pople, J. A. GAUSSIAN86; Carnegie-Mellon Quantum Chemistry Publishing Unit: Pittsburgh, PA, 1984.

Table II. Relative Energies of Methylcarbene, Dimethylcarbene, Cyclohexylidene, Carbena-2-norbornane, Carbena-2-norbornene, and Brexan-5-ylidene and the 1,2-Shift Transition States (Energies Reported (kcal/mol) with all Computed Activation Energies Corrected with Zero-Point Energies from Table I)

species	sym	AM1	3-21G	6-31G*	MP2/6-31G*	$E_{\mathrm{a(EXP)}}$	$\Delta G^{\ddagger}_{\mathrm{rel}}$
methylcarbene	C_1	0.0	0.0	0.0	0.0		
TS H 1,2-shift	C_1	14.0	19.9	12.5	0.9	0.6[a], 1.1 ± 1[b]	
dimethylcarbene	C_s		0.0	0.0	0.0		
dimethylcarbene[c]	C_{2v}	0.0	0.0	0.3	0.4		
dimethylcarbene[d]	C_{2v}	2.3	1.2	1.2	2.1		
TS H 1,2-shift	C_1	18.9	24.9	18.4	6.0	4.7[e]	
cyclohexylidene	C_s	0.0	0.0	0.0	0.0		
TS-ax	C_1	15.8	19.4	12.7	−0.1		0.0
TS-eq	C_1	16.0	19.6	12.8	0.0		0.2[f]
cyclohexylidene[g]	C_1	0.9	0.0	0.0	0.0		
TS-eq[g]	C_1	17.8	22.3	15.4	2.4		
TS-ax[g]	C_1	17.0	21.4	14.7	1.5		
carbena-2-norbornane	C_1	0.0	0.0				
TS-exo	C_1	22.5	26.5				0.0
TS-endo	C_1	22.5	28.3				1.8[h]
carbena-2-norbornene	C_1	0.0	0.0				
TS-exo	C_1	22.8	28.5			0.0	0.0
TS-endo	C_1	22.8	30.6			2.4–2.7[i]	1.5[j], 2.7[k]
brexan-5-ylidene	C_1	0.0	0.0				
TS-exo	C_1	21.7	25.6				0.0
TS-endo	C_1	22.8	28.4				2.9[l]

[a] Reference 18. [b] Stevens, I. D. R.; Liu, M. T. H.; Soundararajan, N.; Paike, N. *Tetrahedron Lett.* **1989**, *30*, 481. [c] CH eclipsed with the CC bond. [d] CH staggered with the CC bond. [e] Best theoretical estimate corrected by the energy difference between MP4/6-311G** and MP2/6-31G* of the methylcarbene rearrangement (0.3 kcal/mol) and the zero-point energy correction (1.5 kcal/mol). [f] Cyclohexylidene at 298.15 K; see ref 5. [g] Constrained optimizations with the axial hydrogen parallel to the vacant p-orbital for the ground-state calculations. Subsequent transition states were determined with the ground-state geometry of the carbon framework held fixed. [h] Dimethylnorbornan-2-ylidene at 298.15 K; see ref 4. [i] Benzonorbornenylidene systems at 463.15 K; see ref 3. [j] Benzonorbornenylidene at 298.15 K; see ref 2. [k] Benzonorbornenylidene at 463.15 K. [l] Brexan-5-ylidene at 298.15 K.

6-31G* and 3-21G basis sets for ab initio calculations[12,13] or with Dewar's semiempirical RHF/AM1 method.[14] Single-point energy calculations were employed to correct for electron correlation with second-order Møller-Plesset perturbation theory.[15] Allinger's MM2 program[16] was used for force-field calculations.

Results and Discussion

There have been several studies of the influence of basis sets and correlation energy on the calculated activation energies for hydrogen 1,2-shifts.[17,18] To further illustrate the effect of theoretical level on these systems, the transition structures of the hydrogen 1,2-shifts in methylcarbene and dimethylcarbene were computed. The results are given in Tables I and II. The MP4/6-311G**//MP2/6-31G* + ZPE estimate of the activation energy of the methylcarbene to ethylene rearrangement has been reported previously as 0.6 kcal/mol.[17] The MP2/6-31G* + ZPE value overestimates the MP4 activation energy by only 0.3 kcal/mol. It is not practical to carry out calculations on the large systems in this study with this high level of theory. However, the 3-21G calculations predict activation energies that are 19.3 kcal/mol higher than those predicted by the MP4 calculations for the methylcarbene rearrangement.[17] To estimate activation energies, 19.3 kcal/mol is subtracted from the 3-21G activation energies calculated for the larger carbenes. This correction factor has been tested for methylcarbene, dimethylcarbene, and cyclohexylidene rearrangements. As shown in Tables I and II, the computed energy differences between RHF/3-21G and MP2/6-31G* are 19.3 kcal/mol for methylcarbene, 18.9 kcal/mol for dimethylcarbene, and 19.5 and 19.6 kcal/mol for the axial and equatorial processes of cyclohexylidene. The error in 3-21G calculations seems to be relatively constant. For the conclusions in this paper, it is only necessary that the relative activation energies of stereoisomeric 1,2-shifts be calculated correctly.

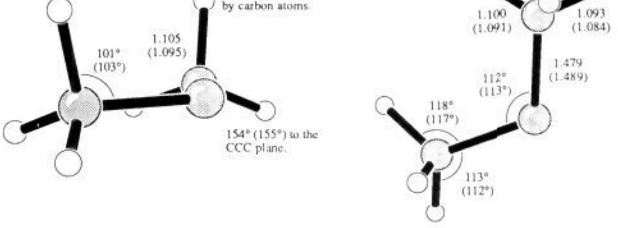

Figure 2. Singlet dimethylcarbene computed at MP2/6-31G* and RHF/6-31G* in parentheses (C_s).

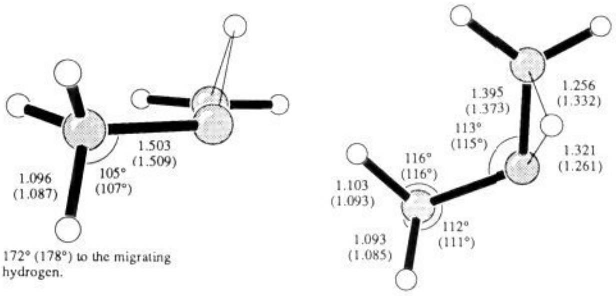

Figure 3. Dimethylcarbene 1,2-shift transition structures computed at MP2/6-31G* and RHF/6-31G* in parentheses.

The C_s structure (Figure 2) is the energy minimum for dimethylcarbene. Significant geometric distortion is observed of the CH bonds best aligned with the vacant p-orbital. The perpendicular CH bond is elongated to 1.105 Å, and the bond angle with the carbene center is compressed to 101°, much smaller than the 113–118° bond angles of the other CH bonds. This is consistent with hyperconjugative interaction of the perpendicular CH bond with the vacant carbene orbital. Two C_{2v} structures are

---

(12) Hariharan, P. C.; Pople, J. A. *Theor. Chim. Acta.* **1973**, *28*, 213.

(13) Binkley, J. S.; Pople, J. A.; Hehre, W. J. *J. Am. Chem. Soc.* **1980**, *102*, 939.

(14) Dewar, M. J. S.; Zoebisch, E. G.; Healy, E. F.; Stewart, J. J. P. *J. Am. Chem. Soc.* **1985**, *107*, 3902.

(15) (a) Møller, C.; Plesset, M. S. *Phys. Rev.* **1934**, *46*, 618. (b) Pople, J. A.; Seeger, R.; Krishman, R. *Int. J. Quant. Chem. Symp.* **1977**, *11*, 49. (c) Krishnan, R.; Pople, J. A. *Int. J. Quantum Chem., Symp.* **1978**, *14*, 91. (d) Krishnan, R.; Frisch, M. J.; Pople, J. A. *J. Chem. Phys.* **1980**, *72*, 4244.

(16) (a) Burkert, U.; Allinger, N. L. *Molecular Mechanics*; American Chemical Society: Washington, D.C., 1982. (b) Allinger, N. L. *J. Am. Chem. Soc.* **1977**, *79*, 8127. (c) Allinger, N. L.; Yuh, Y. H. Molecular Mechanics II; QCPE No. 395; Indiana University, Bloomington, IN 47405.

(17) Evanseck, J. D.; Houk, K. N. *J. Phys. Chem.* **1990**, *112*, 5518.

(18) Krishnan, R.; Frisch, M. J.; Pople, J. A. *Chem. Phys. Lett.* **1982**, *85*, 145.

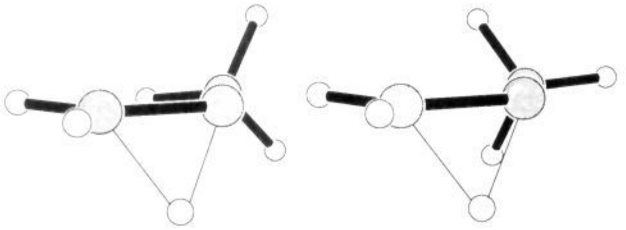

Figure 4. Transition structure for the hydrogen 1,2-shift in methylcarbene (left) and energy maximum for the methyl rotation (right).

second-order saddle points. The one with a CH of each methyl eclipsed with a CC bond is 0.6 kcal/mol above the minimum, and that with staggering of both methyl groups is 1.8 kcal/mol above the minimum.

The RHF and MP2 dimethylcarbene transition structures are shown in Figure 3. The MP2 breaking and forming CH bond lengths are 1.256 and 1.321 Å, and the RHF are 1.332 and 1.261 Å. This is consistent with an earlier transition structure for the reaction when correlation energy is included, which is similar to other comparisons of RHF and MP2 geometries for hydrogen 1,2-shifts.[17,18] With use of the RHF/3-21G correction factor for the activation energy (19.3 kcal/mol) and the calculated zero-point energy correction (0.5 kcal/mol), the 3-21G dimethylcarbene rearrangement is predicted to have an activation energy of 5.6 kcal/mol. This approximation, which is applied to the larger carbene systems in this study, yields satisfactory agreement with the computed MP2 activation energy of 6.0 kcal/mol.

While the migrating hydrogen has advanced much less than 50%, the carbon skeleton and the two hydrogens attached to the migrating origin are all nearly planar, as in the reaction product. Indeed, the transition structure appears to be approximately a hydrogen atom coordinated to a 1-methylvinyl radical. Another observation is that the dipole moment increases from 1.89 D in the ground-state structure to 2.23 D in the transition structure. The methyl substituent rotates in order to realign a hydrogen more or less in an antiperiplanar fashion with the partial bond to the migrating hydrogen. This achieves approximate staggering of the methyl CH bonds with the partial CH bond and also places the methyl group in a conformation like that of the propene product. This is shown more clearly in the Newman projections in Figure 4 and is sketched below.

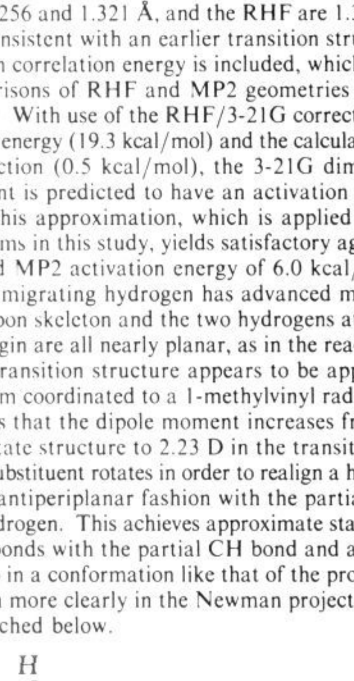

The barrier to rotation of the methyl group was further investigated with partial optimizations. The optimized 3-21G transition structure was held fixed, the dihedral angle between a methyl CH bond and the partially formed bond was fixed at various values, and the positions of the other two methyl hydrogens were fully optimized. An energy maximum of 1.3 kcal/mol occurs upon a 60° rotation. A barrier of about 2 kcal/mol, the same as that of propene, is expected for a methyl group on the other terminus. Torsional preferences in the transition structure will be shown later to have an influence on the rates of rearrangements in rigid polycyclic systems.

Singlet cyclohexylidene was optimized at the RHF/6-31G* level. The structure is shown in Figure 5. The axial hydrogen is only 2° away from perfect coplanarity with the vacant p-orbital of the carbene. The equatorial hydrogen has a dihedral angle of 159°, apparently poorly aligned for migration. The axial hydrogen bond is slightly longer (1.099 Å) than the equatorial (1.086 Å), and the axial hydrogen angle with the carbene atom is compressed to 100°, as compared to 110° for the equatorial.

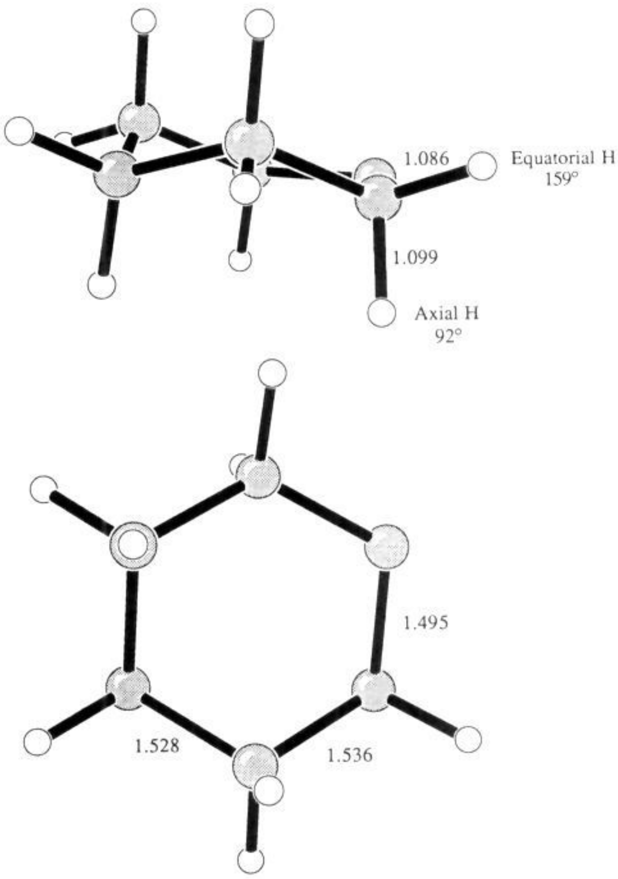

Figure 5. Singlet cyclohexylidene (RHF/6-31G*).

The 6-31G* transition structures for axial and equatorial hydrogen migrations are shown in Figures 6 and 7. The axial transition structure has the CH bond at the migrating origin equal to 1.315 Å and the CH bond at the terminus equal to 1.279 Å. A high degree of planarity has been achieved at the origin of migration, which is reflected in the dihedral angles of the equatorial hydrogen (180°) and the migrating axial hydrogen (104°). The double Newman projection is shown below, along with the torsional angles with values less than 60°.

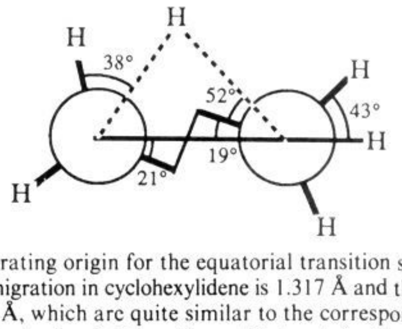

The migrating origin for the equatorial transition structure of hydrogen migration in cyclohexylidene is 1.317 Å and the terminus is at 1.280 Å, which are quite similar to the corresponding axial values. The torsional interactions of interest for the equatorial transition structure are given below. There are considerable similarities with the axial transition structure for the forming and breaking bond, but the ring becomes slightly flattened as shown

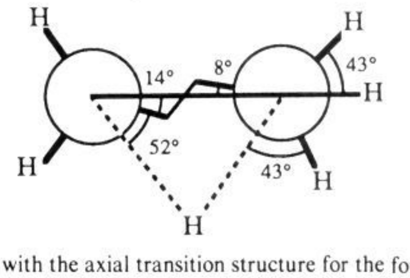

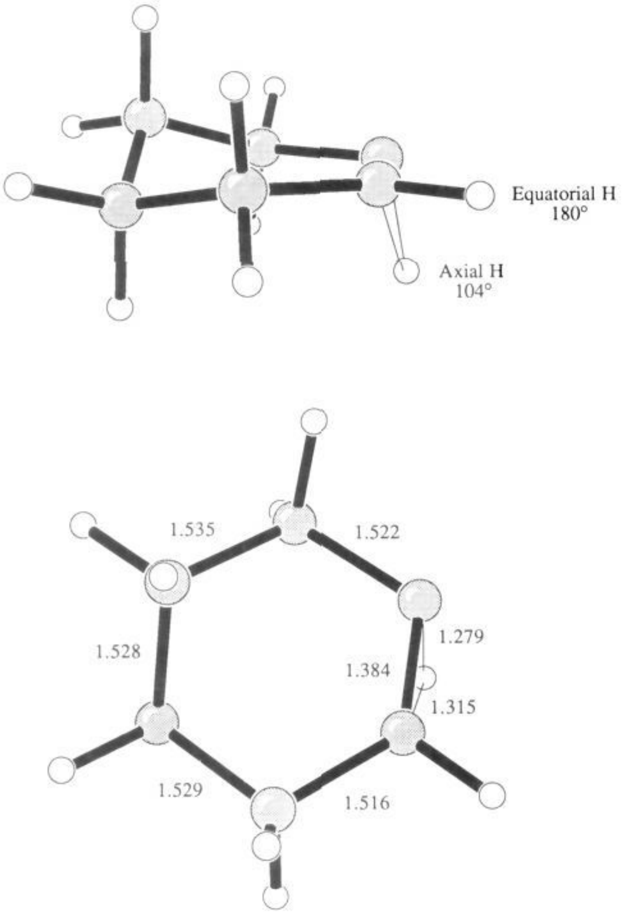

Figure 6. Cyclohexylidene axial transition structure (RHF/6-31G*).

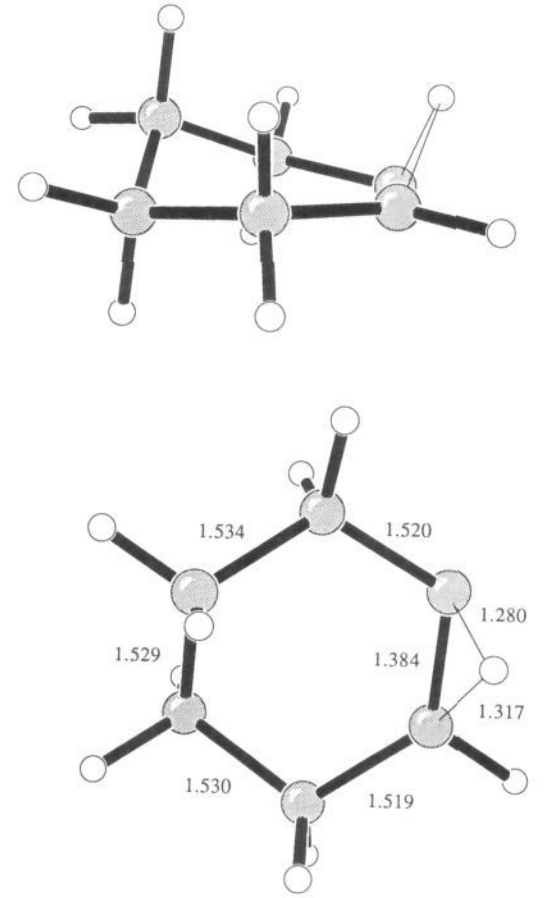

Figure 7. Cyclohexylidene equatorial transition structure (RHF/6-31G*).

by the 8° and 14° torsional angles as compared to the 19° and 21° torsional angles found in the axial structure. Other key geometric similarities include the 52° torsional angle formed between the migration origin and carbon skeleton, the CH alignment with the partially formed bond (43° vs 38°), and the migrating terminus CH torsional angles of 43° in both cases.

Both transition structures resemble a half-chair cyclohexene very closely. Although alignment of the axial and equatorial hydrogens is very different in the reactants, in the transition structures the molecule distorts to nearly the same geometry regardless of which hydrogen migrates. This is in accord with Kyba's conclusions from MNDO calculations.[10]

The axial activation energy is determined to be 0.1–0.2 kcal/mol lower than the equatorial activation energy (Tables I and II). MP2 + ZPE yields 0.0 and −0.1 kcal/mol for the equatorial and axial activation energies, respectively. The correction factor derived for RHF/3-21G calculations plus zero-point energy corrections reduce the 3-21G activation barriers to 0.3 and 0.1 kcal/mol, very close to the values from direct calculations.

To better understand how a rigid framework might influence rates, the axial hydrogen of cyclohexylidene was constrained to be co-planar with the empty carbene p-orbital and the rest of the molecule was allowed to relax. The constrained system was found to have the same energy as the C_s system, which is reasonable, since the original deviation was only 2°. The resulting geometry of the carbon skeleton was held fixed, and the axial and equatorial transition structures were determined with all hydrogen positions fully optimized. Increases in activation energies were observed for both transition structures, at all levels of theory investigated (Tables I and II). The equatorial transition structure is destabilized to a greater extent than the axial transition structure. The energy difference ranged from 0.7 to 0.9 kcal/mol when constrained, as compared to only 0.1–0.2 kcal/mol for the fully optimized system. The key to this very small degree of discrimination is the near-planarity (in the transition structure) of the carbon skeleton framework on which the migration occurs. Because of this, the difference between the axial and equatorial hydrogens is mostly eliminated in the transition structures.

Since the relative energy differences between the axial and equatorial transition states are similar for RHF/3-21G and MP2/6-31G* calculations for cyclohexylidene, only the 3-21G basis set was used to investigate the other systems of interest. The optimized RHF/3-21G singlet-state structure of carbena-2-norbornane is shown in Figure 8. The exo hydrogen is 19° away from perfect alignment for migration, while the endo hydrogen is far away with a dihedral angle of 135°. There is very different alignment of the exo and endo hydrogens of norbornane, contrary to earlier assumptions.[2,3] The exo CH bond is longer (1.092 Å) than the endo CH bond (1.082 Å). The exo CH bond forms a 104° angle with the carbene center, 8° smaller than the corresponding endo angle.

The RHF/3-21G exo transition structure is shown in Figure 9. The structure is observed to be significantly later than others in this study, as reflected by the 1.399-Å migrating origin and 1.289-Å terminus lengths. For comparison, the RHF/3-21G axial cyclohexylidene transition-structure distances are 1.343 and 1.312 Å. The torsional angles involving the migrating hydrogen for this exo transition structure are 26° and 35°. The torsional angle

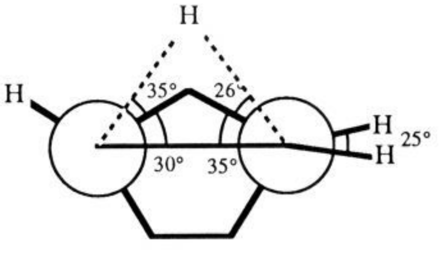

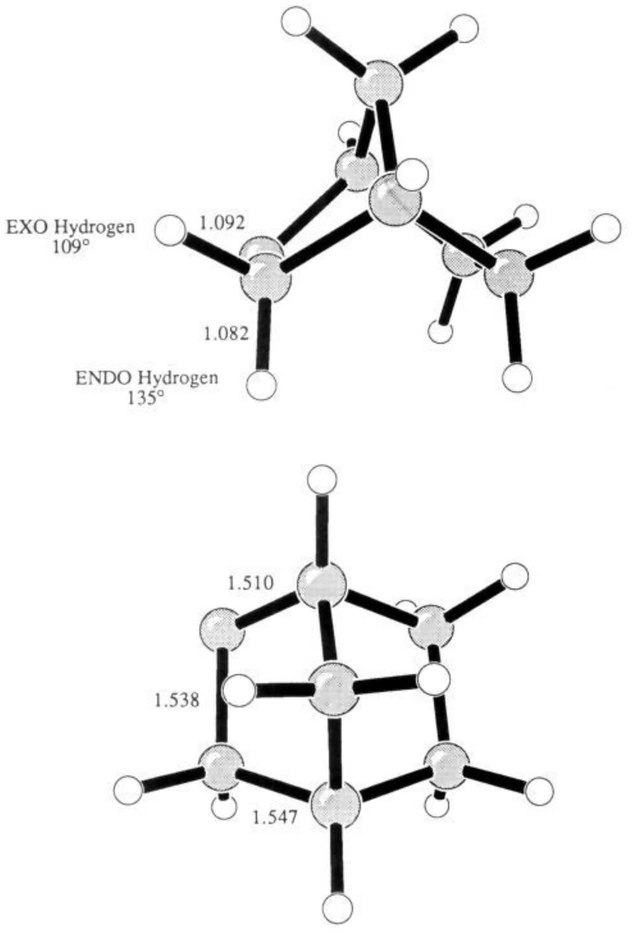

Figure 8. Singlet carbena-2-norbornane (RHF/3-21G).

between the CH bond at the migration origin and adjacent bridgehead carbon atom is 25°. The computed activation barrier at RHF/3-21G is 28.8 kcal/mol (Tables I and II), which after correction is 7.2 kcal/mol.

The migrating origin and terminus lengths are 1.339 and 1.323 Å (Figure 10) in the endo transition structure. The torsional interactions for the endo hydrogen migration process are larger than those for the corresponding exo process. The partial bonds to the migrating hydrogen have significant eclipsing (8° and 9°) with the norbornane CC bonds, as shown below. The CH at the bridgehead is also more nearly eclipsed with the CH bond at C3. The computed RHF/3-21G activation energy for the *endo*-carbena-2-norbornane is 30.6 kcal/mol (Tables I and II). The corrected activation energy prediction is 9.0 kcal/mol, 1.8 kcal/mol higher than that for the exo migration.

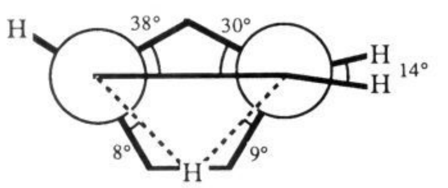

Exo stereoselectivity in additions to substituted norbornenes has been rationalized by Schleyer in terms of torsional interactions.[19] Attack from the exo face should be favored since pyramidalization of the C2 and C3 carbons would increase the torsional interaction (angle α) shown below. Endo attack causes increased eclipsing of the torsional angle α, leading to destabilization.

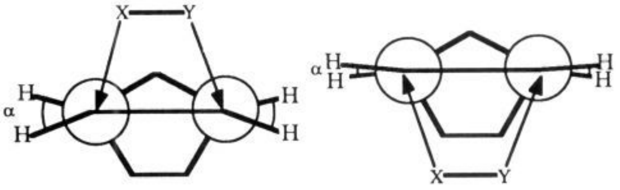

exo attack *endo* attack

Houk et al.[20] later demonstrated that the high thermal addition reactivity on the exo face of *syn*-sesquinorbornene, and of other norbornene reactions, is due to the minimum torsional interactions in the transition structures involving partially formed bonds in addition to these interactions noted earlier by Schleyer.

These same interactions differ in the hydrogen shifts studied here. Eclipsing in the endo transition structures is larger than that in the exo. This difference, rather than the difference in ground-state orbital alignment, is the origin of exoselectivity in these types of systems.

The singlet-state carbena-2-norbornene structure is shown in Figure 11. The exo hydrogen is 20° away from collinear alignment with the vacant carbene p-orbital, while the endo hydrogen forms an unfavorable dihedral angle of 133°. The exo and endo CH bond lengths are 1.090 and 1.080 Å, with angles of 106° and 112° to the carbene center, respectively.

Figure 12 illustrates the exo transition structure for the hydrogen migration in carbena-2-norbornene. The migrating origin is 1.385 Å, and the terminus is 1.301 Å. Again, the migrating hydrogen is free of serious torsional interactions, as shown below. The computed 3-21G activation energy is 30.9 kcal/mol. The prediction for the *exo*-carbena-2-norbornene rearrangement activation barrier is 9.2 kcal/mol.

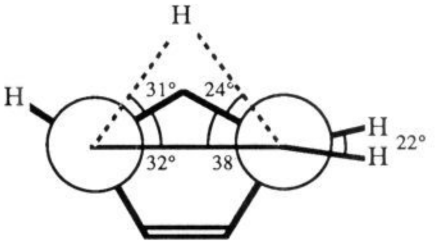

The endo transition structure has a migration origin length of 1.352 Å and terminus of 1.130 Å (Figure 13). Significant eclipsing (1° and 4°) is predicted for the endo process. The corrected activation energy for this endo process is 11.3 kcal/mol, which is 2.1 kcal/mol above that for the exo migration. The larger difference in activation energies can be attributed to the larger difference in torsional interactions in the transition structures.

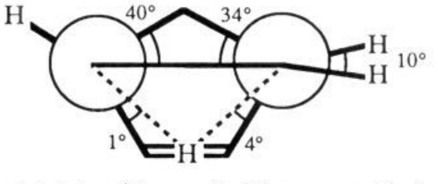

The singlet state of brexan-5-ylidene was optimized at the RHF/3-21G level and is shown in Figure 14. The exo hydrogen is 6° closer to the ideal alignment for migration as compared to the exo hydrogen in carbena-2-norbornane. Correspondingly, the endo hydrogen is twisted 6° toward poorer positioning with respect to the vacant carbene orbital. The exo CH bond distance is 1.094 Å as compared to the endo length of 1.082 Å. The exo hydrogen angle with the carbene carbon is 9° smaller than that found for the endo hydrogen (113°).

The exo transition structure for hydrogen migration in brexan-5-ylidene is shown in Figure 15. The migrating origin (1.392

---

[19] Schleyer, P. v. R. *J. Am. Chem. Soc.* **1967**, *89*, 701.

[20] Houk, K. N.; Rondan, N. G.; Brown, F. K.; Jorgensen, W. L.; Madura, J. D.; Spellmeyer, D. C. *J. Am. Chem. Soc.* **1983**, *105*, 5980.

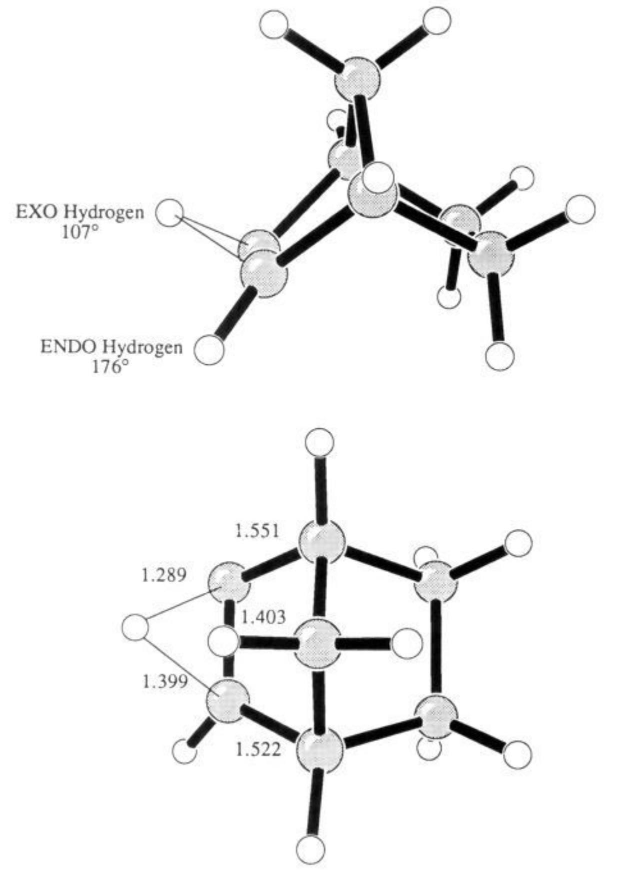

Figure 9. Carbena-2-norbornane exo transition structure (RHF/3-21G).

Å) and terminus (1.294 Å) closely resemble the distances in carbena-2-norbornane.

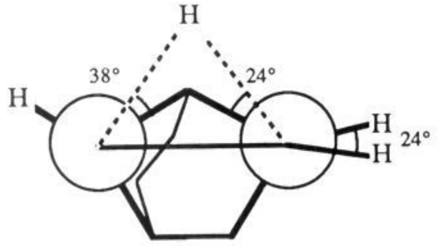

Figure 16 illustrates the endo transition structure for hydrogen migration in brexan-5-ylidene. Consistent with other transition structures, the lengths of the migrating origin (1.335 Å) and terminus (1.323 Å) indicate a more advanced transition state than for the equatorial transition state for cyclohexylidene. Severe torsional interactions are also observed for this endo transition structure. The predicted activation barriers for brexan-5-ylidene are 6.3 and 9.1 kcal/mol for the exo and endo processes, respectively (Tables I and II). The larger selectivies here cannot all arise from differences in torsional interactions (cf. brexan-5-ylidene), since they are somewhat smaller than in the norbornenyl case.

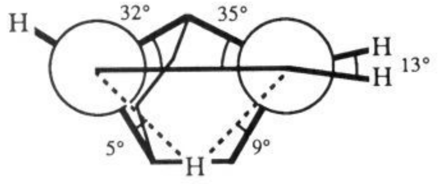

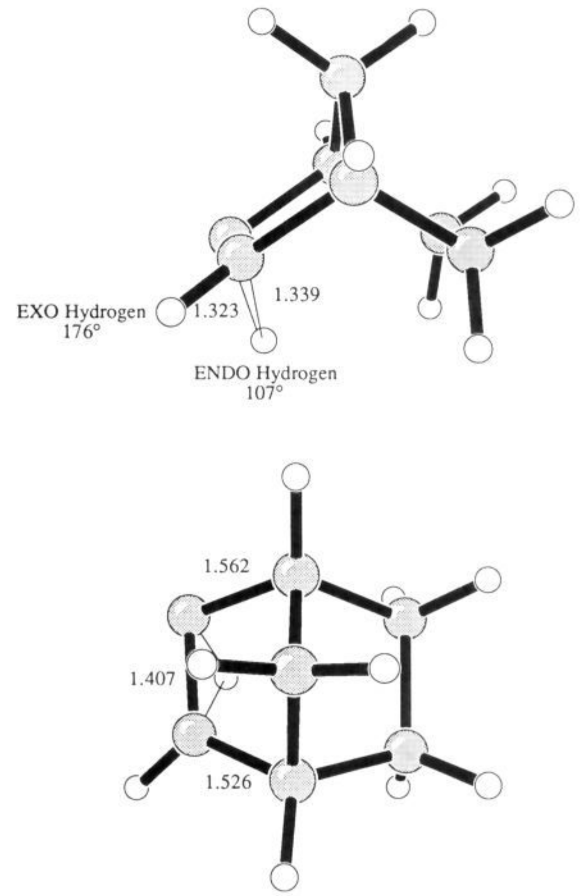

Figure 10. Carbena-2-norbornane endo transition structure (RHF/3-21G).

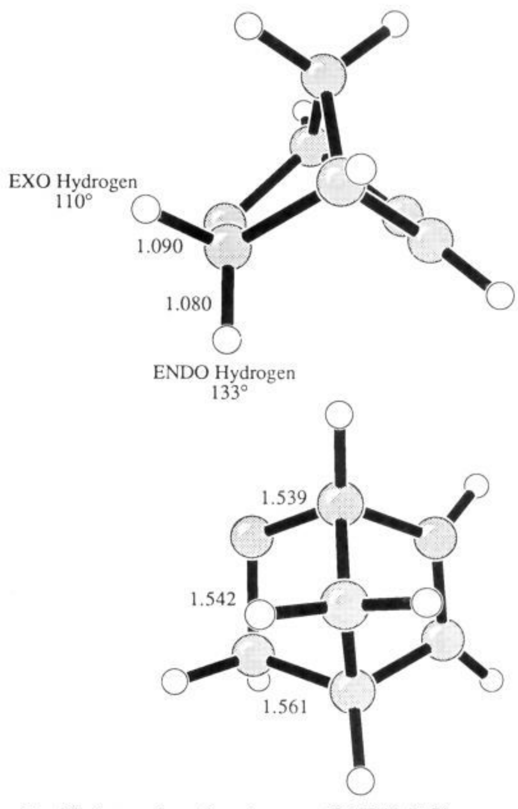

Figure 11. Singlet carbena-2-norbornene (RHF/3-21G).

To explain the enhanced selectivity in reactions of brexan-5-ylidene, we investigated the nonbonded steric interactions that occur at the transition structures. The MM2 program was used to compute nonbonding interactions for the carbenes of interest.[16] No special parameterization was implemented for either the

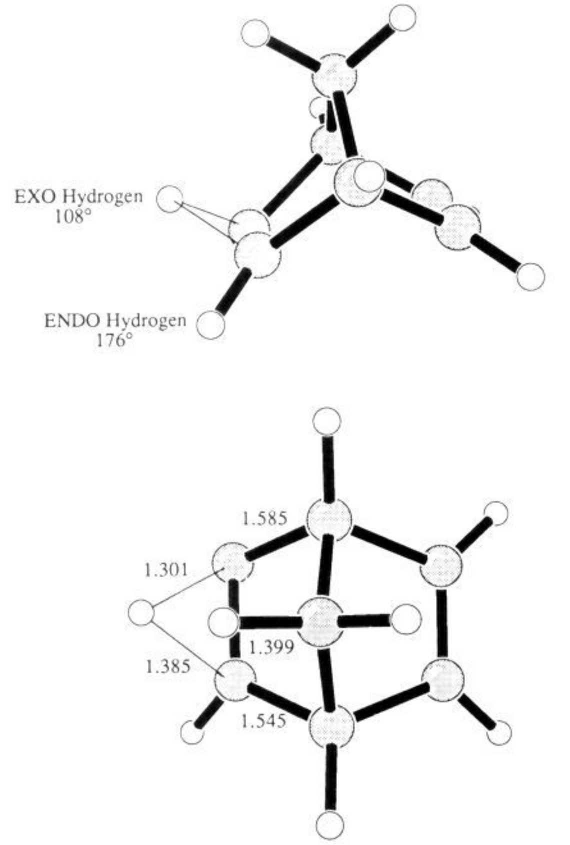

Figure 12. Carbena-2-norbornene exo transition structure (RHF/3-21G).

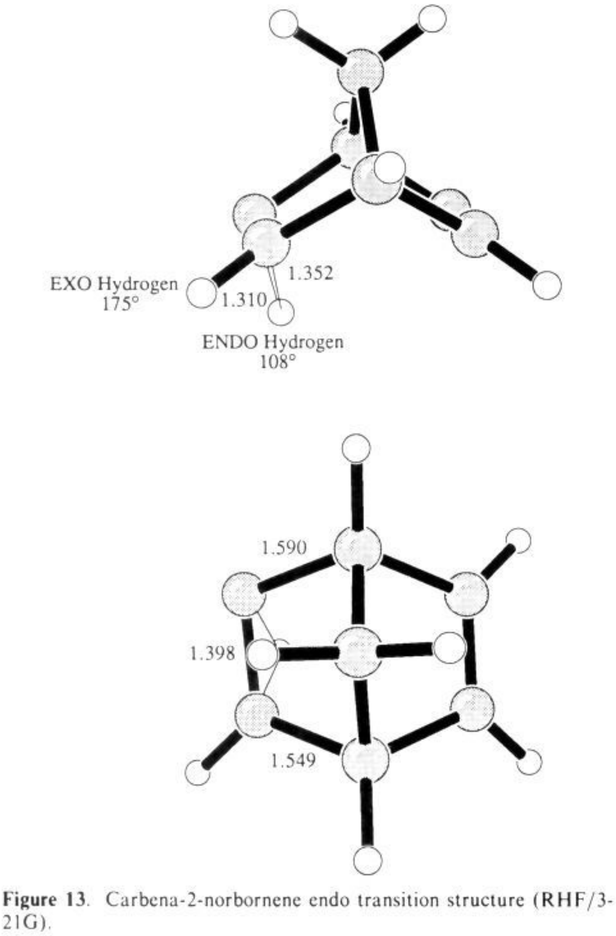

Figure 13. Carbena-2-norbornene endo transition structure (RHF/3-21G).

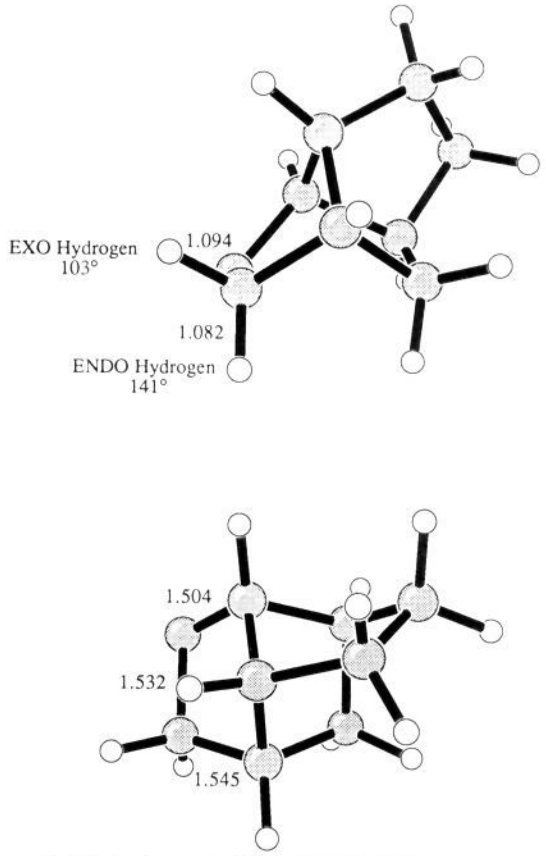

Figure 14. Singlet brexan-5-ylidene (RHF/3-21G).

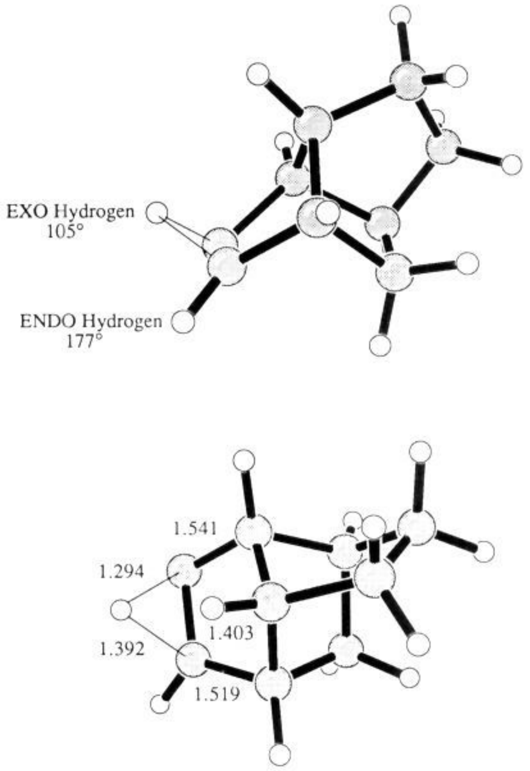

Figure 15. Brexan-5-ylidene exo transition structure (RHF/3-21G).

ground or transition structures, and geometries were fixed at their 3-21G values. The distance between the hydrogen at the C7 position and the migrating exo hydrogen in the brexan-5-ylidene system is 0.11 Å longer than the distance in carbena-2-norbornane. MM2 calculations give van der Waals energy of 0.3 kcal/mol for

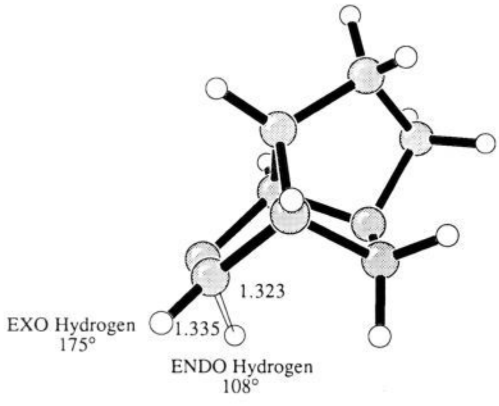

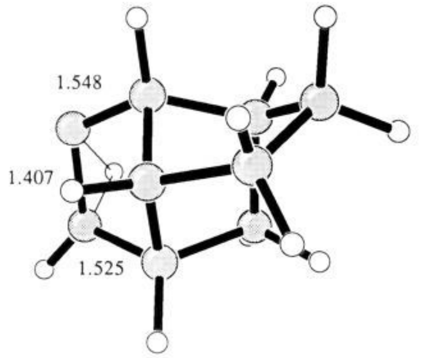

Figure 16. Brexan-5-ylidene endo transition structure (RHF/3-21G).

this interaction, as compared to the 0.4 kcal/mol computed for carbena-2-norbornane. The closest nonbonded hydrogen interaction distance involving the migrating endo hydrogen is 2.30 Å for the brexan-5-ylidene endo transition structure and 2.58 Å for carbena-2-norbornane. The MM2 van der Waals energies are 0.7 and 0.1 kcal/mol, respectively. There is 0.4 kcal/mol less nonbonded replusion in the exo transition structure of brexan-5-ylidene than in the endo transition structure. This exo preference is 0.7 kcal/mol larger than in carbena-2-norbornane.

Conclusion

Ground-state alignment has little influence on the rates of hydrogen 1,2-shifts in carbenes. The significant eclipsing of the partial bonds that develops in the endo transition structures is thought to be the origin of exo selectivity in the norbornane structures. The twist induced by the additional ethane bridge in brexan-5-ylidene modifies the alignment of the exo and endo hydrogens, along with the nonbonded interaction sites that are found to determine the unusually high selectivity of this system. Theoretical calculations predict the exo (axial) and endo (equatorial) activation barriers of larger carbene systems: dimethylcarbene (6.0 kcal/mol), cyclohexylidene (−0.1 and 0.0 kcal/mol), carbena-2-norbornane (7.2 and 9.0 kcal/mol), carbena-2-norbornene (9.2 and 11.3 kcal/mol), and brexan-5-ylidene (6.3 and 9.1 kcal/mol). Because tunneling will enhance rates of hydrogen shifts in carbenes, measured barriers may prove to be even lower than these.[21]

Acknowledgment. We are grateful to the National Science Foundation for financial support of this research and to Professor Alex Nickon of Johns Hopkins University for helpful discussions. This work was supported in part by a grant of computer time made possible under a joint study with the IBM Corp. on the IBM 3090/600J Supercomputer at the UCLA Office of Academic Computing. Dr. Michael Miller provided the graphics for Figures 2–16.

---

(21) Osamura, Y.; Schaefer, H. F., III; Gray, S. K.; Miller, W. H. *J. Am. Chem. Soc.* **1981**, *103*, 1904. Gray, S. K.; Miller, W. H.; Yamaguchi, Y.; Schaefer, H. F., III. *Ibid.* **1981**, *103*, 1900.

Electron Affinity of O^- and Diabatic CaO(g) Integer Charge Potential Curves

David P. Baldwin,*,[†] Ernest J. Hill, and Robert W. Field

Contribution from the George R. Harrison Spectroscopy Laboratory and the Department of Chemistry, Massachusetts Institute of Technology, Cambridge, Massachusetts 02139.

Received April 13, 1990

Abstract: A ligand field, integer-charge ionic model for the electronic structure of diatomic CaO(g) provides a basis for an empirical deperturbation of the lowest lying $^1\Sigma^+$ electronic states to their diabatic doubly charged ($Ca^{2+}O^{2-}$) and singly charged ionic (Ca^+O^-) potentials. The deperturbed doubly charged and lowest singly charged potentials cross at $r_{\text{Ca-O}} = 2.16$ (1) Å at an energy 10 400 (100) cm^{-1} above $v = 0$ of the experimentally observed $X^1\Sigma^+$ ground state. The interaction matrix elements between the three lowest interacting $^1\Sigma^+$ states have been determined as functions of $r_{\text{Ca-O}}$. With use of a simple Rittner model for the diabatic curves, extrapolation to infinite internuclear separation yields a value for the electron affinity of O^- (i.e., $O^- + e^- \rightarrow O^{2-}$) of −4.53 (6) eV, in agreement with quantum-chemical results, and a value of 35 160 (200) cm^{-1} for D_0^0 of CaO, in excellent agreement with thermochemical values.

I. Introduction

The electronic spectra of the fourth-row, gas-phase, diatomic metal oxides are among the most complicated and congested diatomic spectra observed. Assignment of transitions and derivation of molecular constants from these spectra, which often contain rovibronic transitions with a spectral density of >10 lines/cm^{-1} over the entire visible region, has largely become possible only with the advent of high resolution, tunable, visible wavelength lasers and multiple resonance and selectively detected excitation techniques. Even with the present ability to derive molecular constants from strongly perturbed and dense spectra, with few exceptions it has not been possible to go beyond the molecular constants of individual electronic states to a global

---

[†] Current address: Combustion Research Facility, Sandia National Laboratories, Livermore, CA.

0002-7863/90/1512-9156$02.50/0